

<https://doi.org/10.1038/s41612-024-00593-6>

# Equatorward shift of the boreal summer intertropical convergence zone in Maritime Continent and the impacts on surface black carbon concentration and public health



Tao Huang<sup>1,2</sup>, Yefu Gu<sup>3</sup>, David Lallemand<sup>2,4</sup>, Gabriel N. C. Lau<sup>5</sup>, Joseph J. Y. Sung<sup>1</sup> & Steve H. L. Yim<sup>1,2,4</sup> ✉

In Maritime Continent, the shift of intertropical convergence zone (ITCZ) location directly regulates the distribution of black carbon and hence affects public health in the region, but the mechanism and human health impacts have not yet been comprehensively revealed. Here we used multiple reanalysis datasets to investigate the long-term shift of seasonal-mean zonal-mean ITCZ location in this region from 1980 to 2014, and to assess the influences on black carbon distribution and the resultant health impact in terms of premature mortality. Results show that recent human-related equatorial warming contributed to an equatorward shift ( $\sim 2.1^\circ$ ) of ITCZ location in Maritime Continent. Spatially, the equatorward shift of ITCZ reduced surface black carbon concentration over the maritime area by enhancing updrafts and wet deposition, but raised the concentration in the continental area by inhibiting updrafts. Meanwhile, anomalous low-level northeasterlies weakened summer circulation and prevented black carbon from being transported to the Philippines. Our results also suggest that the equatorward shift decreased  $\sim 13\%$  of black carbon-associated monthly premature mortality in maritime countries, but increased  $\sim 6\%$  of that in continental countries based on the population and mortality rate in 2010. We therefore recommend considering climate change impacts in the design of adaptation strategies against regional air pollution.

The intertropical convergence zone (ITCZ) plays an essential role in regulating weather and climate regionally and globally. The location of ITCZ not only dominates the atmospheric circulation in the deep tropics directly, but also influences regions at high latitudes through Hadley cells<sup>1–5</sup>. By its nature, the ITCZ location follows the position where the column-integrated meridional energy flux vanishes (i.e., energy flux equator)<sup>2</sup>, travelling from the Southern Hemisphere to the Northern Hemisphere from boreal winter to summer<sup>6–9</sup>. The climatology and variability of ITCZ location in the past and in a warming future inevitably have huge impacts on the circulation

patterns, hence the redistribution of air pollutants and public health<sup>5,10,11</sup>. Discussion has been lasting for over a decade but many conclusions about the impacts of ITCZ shift still remain debatable in terms of different spatiotemporal scales<sup>12,13</sup>.

Seasonal-mean zonal-mean ITCZ location indicates the position of the ascending branch of Hadley circulation<sup>2,3</sup>. It is typically defined as the latitude of the ascent peak averaged over the corresponding longitude range in a particular season instead of in a whole year<sup>1,12</sup>. Past studies evidently pointed out that the seasonal ITCZ location better reveals ITCZ dynamics than the

<sup>1</sup>Lee Kong Chian School of Medicine, Nanyang Technological University, Singapore, Singapore. <sup>2</sup>Earth Observatory of Singapore, Nanyang Technological University, Singapore, Singapore. <sup>3</sup>Department of Geography and Resource Management, The Chinese University of Hong Kong, Sha Tin, 999077 Hong Kong, China. <sup>4</sup>Asian School of the Environment, Nanyang Technological University, Singapore, Singapore. <sup>5</sup>Geophysical Fluid Dynamics Laboratory/NOAA, Princeton University, P.O. Box 308, Princeton, NJ, USA. ✉e-mail: [yimsteve@gmail.com](mailto:yimsteve@gmail.com)

annual one because it depicts the physical meaning of the convergent belt more accurately<sup>1,12</sup>. For example, some dominating seasonal location migrations led by Earth energy budget variations are easily neglected in an annually averaged result<sup>14</sup>, failing to provide a full review of the ITCZ dynamics<sup>12</sup>. Although many researchers believe that an annual scale expansion of the tropics is happening<sup>15–19</sup>, the long-term variations of seasonal-scale deep-tropical ITCZ location still remain uncertain under the effects of both natural variability and anthropogenic activities<sup>6,20,21</sup>.

Although prior findings are still debatable, zonal variation of ITCZ location is manifested clearly<sup>3,9</sup>. From a global perspective, ITCZ will shift poleward because of a potentially warming Northern Hemisphere due to anthropogenic activities-induced drought and albedo loss<sup>22–24</sup>. However, questions about regional distinctions arise when contrasting shifts of ITCZ location in different regions have been captured in both historical observations and in climate projections. For example, among the ensemble mean results derived from 27 CMIP6 models, both Eastern Africa and the Indian Ocean show a northward shift ITCZ location whereas the Eastern Pacific and the Atlantic Oceans turn out an opposite change<sup>9</sup>. Distinctions and uncertainties also stem from different datasets and methodologies (i.e., maximum precipitation, highest ongoing longwave radiation used in different reanalysis datasets) used to define the location of ITCZ<sup>4,7,8,12,13</sup>. Recent studies have pointed out that divergent atmospheric energy transport may be a potential driver that determines the latitude of ITCZ zonally<sup>3,9</sup>. In general, prior studies highlight the importance of a regional-scale investigation of ITCZ shifts under climate change.

The Maritime Continent acts as the heat source for the entire global circulation system and is easily affected by the location of ITCZ<sup>25,26</sup>. It has also become one of the major aerosol sources in the globe because severe haze events from wildfires and anthropogenic biomass burning have occurred during the past decades frequently<sup>27–30</sup>. For example, in a single year of 1997, biomass burnings over the Indonesia produced about 11 percent of the global total carbon emission<sup>25,31</sup>. Among the emitted carbon products, black carbon (BC) was found to be associated with multiple adverse health impacts especially for the premature mortality under both long-term and short-term exposures<sup>32–34</sup>. Given the pronounced health risk, the assessments of the health impacts of BC in Maritime Continent are still lacking, especially when the BC concentration is substantially affected by ITCZ location<sup>35</sup>. Here, we used multiple reanalysis datasets and CMIP6 simulations to comprehensively investigate the long-term shift of seasonal ITCZ location in Maritime Continent from 1980 to 2014, and linked this shift to anthropogenic greenhouse gas emissions. Further, we analysed the influence of ITCZ shift on BC concentration from the atmospheric

circulation perspective, and finally assessed its health impact in Maritime Continent. This study aims to understand the role of climate change in regional air pollution regulation and to provide an essential reference for the government in the future mitigation of environmental problems.

## Results

### Recent equatorward shift of ITCZ location in Maritime Continent

In boreal summer (June–September, 1980–2014), regional zonal-mean ITCZ was typically located at  $\sim 10^\circ\text{N}$  over Maritime continent (Supplementary Fig. 1). ITCZ shifted equatorward by  $\sim 2.1^\circ$  in the recent decade (2005–2014) compared with that in the historical decade (1980–1989), revealed significantly ( $p < 0.001$  in Student's t-test) in all four datasets (Fig. 1a). Also, a significant linear trend of equatorward ITCZ shift (Supplementary Fig. 2,  $-0.08^\circ$  per year,  $p < 0.05$  in each dataset) was detected from 1980 to 2014. Meanwhile, the intensity of ITCZ increased significantly by  $\sim 0.016 \text{ Pa s}^{-1}$ . It is noted that the width of ITCZ did not change significantly (Supplementary Table 1). One explanation is that the shape of ITCZ in Maritime Continent is not as regular as the shape over the oceans (i.e., a narrow belt) due to the heating and moisture differences induced by land areas, from which the expansion of the ITCZ boundaries cannot be detected evidently (see the Methods section). The result of ITCZ shift in Maritime Continent was different from those showing a poleward shift of ITCZs in Southern, Eastern and Central Pacific where the atmosphere over the oceans could be affected by Pacific Decadal Oscillation (PDO) significantly<sup>12</sup>, highlighting the zonal contrasting shifts of ITCZ under climate change<sup>9</sup>.

Equatorial warming contributes to the equatorward shift of global deep tropical contraction under future climate change<sup>1</sup>. On regional scale, the probability of a warming SST anomaly in the equatorial region ( $5^\circ\text{S}$  to  $5^\circ\text{N}$ ) of Maritime Continent increased by around three-fold in the recent decade compared to that in the historical one (Supplementary Fig. 3). Our study shows that a warmer regional equatorial SST anomaly in the recent decade was significantly associated with a regional equatorward shift of ITCZ location (Fig. 1b). This is consistent with the findings in previous studies that focused on future warming. This pinpoints that equatorial warming contributed to the recent equatorward shift of ITCZ in Maritime Continent, and the contribution is highly possible to continue in the future.

To further point out the contribution of anthropogenic activities to the recent regional equatorial warming in Maritime Continent, we selected 10 models from the CMIP6 with both All-hist and Nat-Hist simulations of near surface air temperature ( $T$ ) and compared the probability density function (PDF) of temperature anomalies among Observation, Nat-hist and All-hist

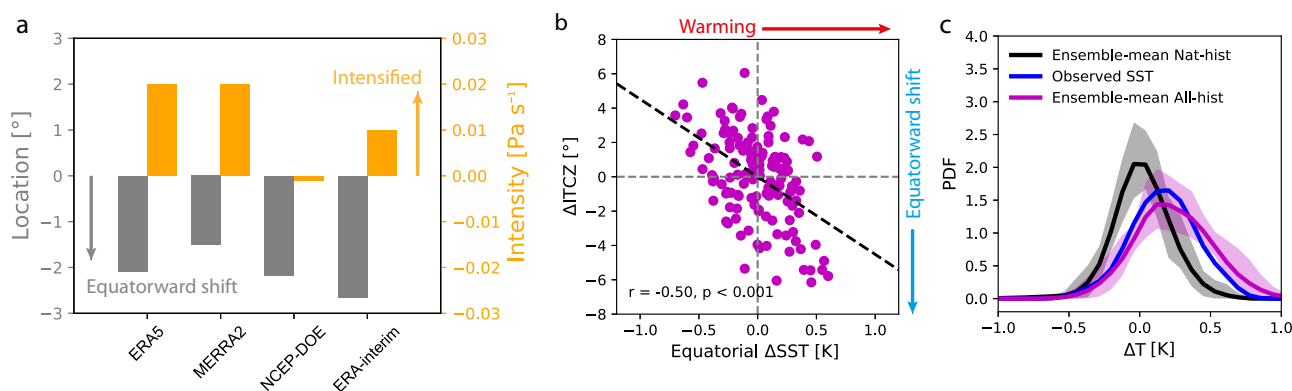


**Fig. 1 | Recent changes of location and intensity of boreal summer ITCZ in Maritime Continent and the association with equatorial warming.** **a** Changes of location (grey bars) and intensity (orange bars) of boreal summer (JJAS) ITCZ over Maritime Continent between recent (2005–2014) and historical (1980–1989) decades derived from  $\omega_{500}$  (Methods) in four reanalysis datasets (ERA5, MERRA-2, NCEP-DOE and ERA-interim). **b** Scatter plot of boreal summer ITCZ location and equatorial ( $5^\circ\text{S}$  to  $5^\circ\text{N}$ ;  $90^\circ\text{E}$  to  $160^\circ\text{E}$ ) SST anomalies from 2005 to 2014.

**c** Attribution of equatorial warming to anthropogenic activities using All-hist and Nat-hist CMIP6 simulations. Black curve refers to the ensemble-mean near surface air temperature anomalies simulated only considering natural forcings, while magenta curve refers to the situation considering all forcings. Blue curve is the observed SST anomalies in the equatorial area. Shading areas refer to the 90% confidence interval among 10 models. Significance ( $p < 0.05$ ) between simulations and observation is tested via Kolmogorov–Smirnov (KS) test.

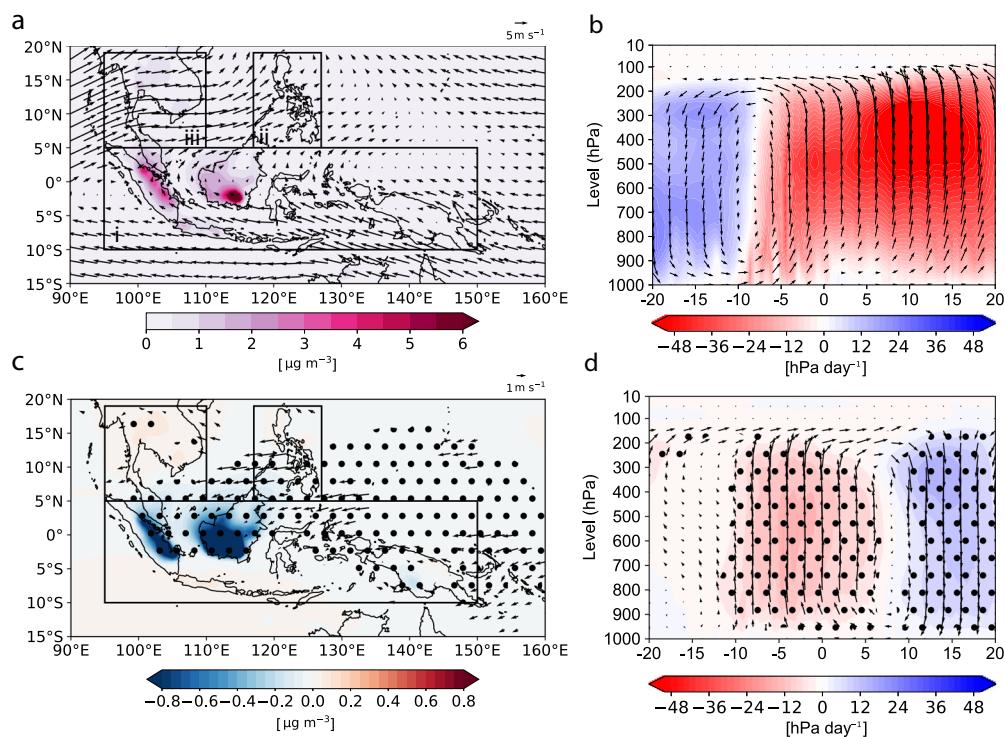


**Fig. 2 | Climatology and composite anomalies of wind and surface BC concentration in boreal summer (JJAS) from 1980 to 2014 in Maritime Continent.** **a** Climatology of boreal summer 850 hPa circulation ( $\text{m s}^{-1}$ ) and surface BC concentration ( $\mu\text{g m}^{-3}$ ) averaged from 1980 to 2014 over Maritime Continent. Black boxes show three sub-regions in Maritime Continent. i: Maritime area; ii: the Philippines; iii: Continental area. Shading refers to near surface BC concentration, whereas vectors show horizontal wind. **b** Climatology of boreal summer regional zonal-mean cross-section of vertical velocity ( $\omega$ ) and meridional wind ( $v$ ) in Maritime Continent averaged from 1980 to 2014.  $\omega$  has been multiplied by 100 for

visualization. Shading refers to the magnitude of  $\omega$  ( $\text{hPa per day}$ ). Red patch represents updrafts. **c** Composites of surface BC concentration and 850 hPa circulation anomalies when ITCZ shifted equatorward ( $\Delta\text{ITCZ} < 0$ ) in boreal summer from 1980 to 2014. Shading refers to the changes of BC concentration, whereas vectors represent circulation anomalies. Stippling stands for statistically significant changes (two-tailed t-test;  $p < 0.05$ ) of BC and only statistically significant wind vectors are shown in the figure. **d** Composites of vertical velocity ( $\omega$ ) and meridional wind ( $v$ ) anomalies when ITCZ shifted equatorward in boreal summer from 1980 to 2014. Stippling stands for statistically significant changes (two-tailed t-test;  $p < 0.05$ ).

situations (Methods). Figure 1c shows that the ensemble-mean PDF from the CMIP6 All-hist simulations described the observed regional equatorial warming well (Methods: KS-test,  $p < 0.05$ ), while the Nat-hist one was significantly cooler than the observed warming signal. It suggests that anthropogenic activities play a vital role in equatorial warming, shifting the ITCZ to the equator in Maritime Continent.

**Impacts of ITCZ shift on black carbon concentration in Maritime Continent**

In boreal summer, the prevailing wind at 850 hPa changed to westerlies in the Northern Hemisphere after travelling across the equator (Fig. 2a). Regional mean surface BC concentration in the maritime area ( $10^{\circ}\text{S} - 5^{\circ}\text{N}$ ,  $95^{\circ}\text{E} - 150^{\circ}\text{E}$ ), the Philippines ( $5^{\circ}\text{N} - 19^{\circ}\text{N}$ ,  $117^{\circ}\text{E} - 125^{\circ}\text{E}$ ) and the continental area ( $5^{\circ}\text{N} - 19^{\circ}\text{N}$ ,  $95^{\circ}\text{E} - 110^{\circ}\text{E}$ ) was  $0.41$ ,  $0.17$  and  $0.36 \mu\text{g m}^{-3}$ , respectively. The maxima occurred in Central Sumatra and Borneo within the maritime area with the value of  $13.4 \mu\text{g m}^{-3}$ , which was around 27 or 10 folds of the maxima in the Philippines ( $0.5 \mu\text{g m}^{-3}$ ) or in the continental area ( $1.28 \mu\text{g m}^{-3}$ ), respectively. In boreal summer from 1980 to 2014, near surface BC concentration was positively correlated with BC biomass burning emission in the maritime area (Supplementary Fig. 4a), and was consistent with the most frequent fire events observed in this area by satellite<sup>25</sup>. However, BC concentrations in the Philippines and the continental area were more associated with other anthropogenic emissions than biomass burning emissions (Supplementary Fig. 4b). Figure 2b shows that updrafts of local Hadley Circulation in boreal summer dominated all three areas. Descent branches were located south to the maritime area in the Southern Hemisphere, transporting dry energy from the Northern Hemisphere to the Southern Hemisphere in upper-level atmosphere<sup>36</sup>.

Figure 2c shows that BC concentration declined significantly in Central Sumatra and Borneo within the maritime area by up to  $\sim 74\%$  ( $-9.88 \mu\text{g m}^{-3}$ ) when ITCZ shifted equatorward (defined as  $\Delta\text{ITCZ} < 0$ , where  $\Delta\text{ITCZ}$  is the monthly ITCZ location anomaly relative to long-term monthly mean from 1980 to 2014). Conversely, BC concentration in the continental area increased by up to  $0.11 \mu\text{g m}^{-3}$  significantly at the same time. This result was consistent with the correlation between time series of ITCZ and BC anomalies from an annual perspective in Supplementary Fig. 5. Significant reduction of BC was only observed in the southern part of Philippines, dominated by significant anomalous easterly or northeasterly low-level (i.e., 850 hPa) winds. It indicates that the weakening of summer monsoon (southwesterlies) inhibited BC transport from Central Sumatra and Borneo to the Philippines through low-level advection when ITCZ shifted equatorward. Figure 2d describes that the significant enhancement of updrafts in the maritime area reduced BC concentration by vertical dispersion. Instead, the suppression of updrafts in the continental area might constrain the BC near the surface and deteriorate air pollution. Supplementary Fig. 6 shows no significant changes of column density of BC in the continental area, indicating that there was not contribution from advection to the increment of BC in this region, whereas the significant reduction of column density in southern part of the Philippines highlights the reduction of transboundary air pollution. Meanwhile, the significant decrease in column density of BC in the maritime area was associated with evident increase in rainfall ( $+ 28 \text{ mm per month}$ ) in this area when ITCZ shifted equatorward (Supplementary Fig. 7). Together with the significant negative correlation between boreal summer precipitation and BC concentration in Supplementary Fig. 8, it indicates that wet deposition was the main way to remove BC from the atmosphere in the maritime area.

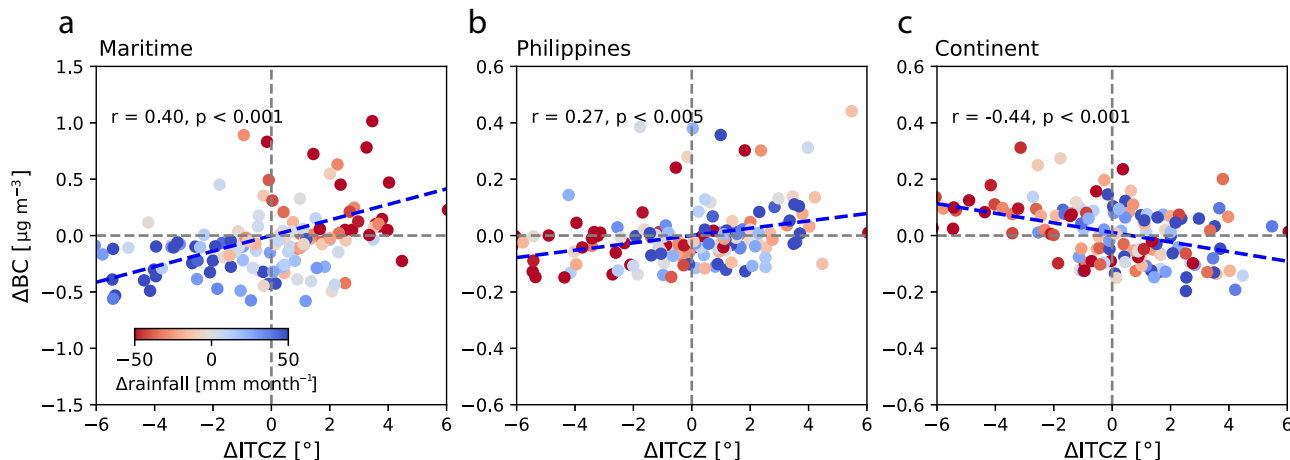


**Fig. 3 | Scatter plots of the relationship between BC changes and ITCZ shift in each region of Maritime Continent.** **a** Maritime area; **(b)** the Philippines and **(c)** Continental area. Colors of dots refer to the regional changes of rainfall. Negative ΔITCZ value refers to the equatorward shift. Extreme ITCZ shift under current equatorial warming is defined as ΔITCZ < -2.1°, which is the extent of shift in the recent decade.

The weakened East Asia Summer Monsoon (EASM) shown in Fig. 2c could be associated with the anomalous western north pacific subtropical high (WNPSH) when ITCZ shifts. Theoretically, a weakening WNPSH strength in boreal summertime can suppress EASM. However, Supplementary Fig. 9 reveals that instead of strength, the position changes of WNPSH might play a more important role in the weakened circulation in southern part of the Philippines. This finding is consistent with the result of an equatorward shift of East Asia Summer Jet and Meiyu-Baiu rainband in Zhou et al. (2019)<sup>1</sup> in early summer time (June and July) during ITCZ equatorward shift period. In a warming future, the WNPSH evolution is still debatable. For example, He and Zhou (2020) utilized CMIP6 simulations and found that the variation in the WNPSH was insignificant and could not strengthen the EASM under global warming scenarios<sup>37</sup>. Similar results were also illustrated in Liu et al. (2018) using 19 CMIP5 models<sup>38</sup>, while an enhanced EASM was detected in a warming climate by Li et al. (2019) using large ensemble simulations with Canadian Earth System Model version 2<sup>39</sup>. In general, the weakened circulation in Fig. 2c should be more related to the position change of WNPSH than intensity change during ITCZ shift period.

Figure 3 further illustrates the relationship among regional BC changes, ITCZ shift and regional rainfall changes in Maritime Continent. In the maritime area, an equatorward shift of ITCZ (ΔITCZ < 0) was associated with an overall decrease of -0.13 μg m<sup>-3</sup> BC concentration. This reduction was more pronounced (-0.21 μg m<sup>-3</sup>) when ITCZ shifted to an extreme situation defined as the shift in recent decade found in Fig. 1 (i.e., ΔITCZ < -2.1°). Rainfall impacts dominated this area, which was proved by the patterns of decrease (increase) rainfall in the first (third) quadrant in Fig. 3a. For the Philippines, the decrease of BC (-0.03 μg m<sup>-3</sup>) during the period with ΔITCZ < 0 was not as pronounced as that in the maritime area. Figure 2c suggests that the suppression of transboundary air pollution played the main role although rainfall decreased during the same period (Fig. 3b), which was supposed to deteriorate the BC concentration. In the continental area, a significant negative correlation occurred between equatorward ITCZ shift (ΔITCZ < 0) and BC increase (+0.05 μg m<sup>-3</sup>). The suppression of vertical dispersion led to such a relationship, confirmed by both anomalous downdrafts in Fig. 2d and rainfall suppression (-20.1 mm per month) in Fig. 3c. The deterioration of BC can be two-times magnified (+0.10 μg m<sup>-3</sup>) when ITCZ shifted to an extreme situation (ΔITCZ < -2.1°).

**Implications for public health**

Based on the population and mortality rate in 2010 and 2015, we further assessed the influence of BC changes induced by ITCZ shift on all-age all-cause premature mortalities in each country in Maritime Continent. Table 1

**Table 1 | Assessment of all-age all-cause premature mortalities in Southeast Asian countries associated with BC based on the population and mortality rate in 2010**

Country	35-year boreal summer mean premature mortality (premature mortalities per month)	95% CI	Percentage change (%) of extra premature mortalities due to ITCZ equatorward shift (+/-)	Percentage change (%) of extra premature mortalities due to extreme ITCZ equatorward shift (+/-)
Indonesia	304	(289, 319)	-12.2	-11.8
Vietnam	98	(93, 103)	5.1	4.1
Thailand	57	(54, 60)	7.0	10.5
Malaysia	27	(26, 28)	-22.2	-29.6
Myanmar	24	(23, 25)	4.2	4.2
Philippines	24	(23, 25)	-4.2	-8.3
Singapore	13	(12, 14)	-23.1	-30.8
Cambodia	11	(10, 11)	9.1	18.2
Timor-Leste	10	(10, 10)	0.0	-10.0
Laos	5	(5, 5)	0.0	0.0
Brunei	1	(1, 1)	0.0	0.0
Maritime	355	(337, 372)	-13.0	-14.1
Continental	195	(185, 205)	5.6	6.7
Overall	574	(545, 601)	-6.1	-6.6

shows that BC-associated monthly mean premature mortalities in boreal summertime were most pronounced in Indonesia [304 (95% CI: 289–319)], Vietnam [98 (95% CI: 93–103)] and Thailand [57 (95% CI: 54–60)]. In maritime countries (i.e., Indonesia, Malaysia, Timor-Leste, Singapore, and Brunei Darussalam), BC led to around 355 (95% CI: 337–372) premature mortalities per month, while in continental countries (i.e., Vietnam, Thailand, Myanmar, Cambodia and Laos), 195 (95% CI: 185–205) monthly premature mortalities were associated with BC, which were around 55% of those in the maritime area. In months with an equatorward shift of ITCZ, nearly 13 percent of the premature mortalities (-46, 95% CI: -48 to -43) could be reduced in maritime countries by the decline of BC concentration via vertical dispersion and wet deposition processes. However, around 6 percent of premature mortalities (11, 95% CI: 11–12) would be induced by the increase of BC in continental countries. In the Philippines, there were

relatively higher monthly premature mortalities associated with BC (24, 95% CI: 23–25), but the changes due to the ITCZ shift was not significant compared to those in other two areas. Totally, the equatorward shift of ITCZ decreased premature mortalities in Maritime Continent by 6 percent during boreal summer, helping to mitigate the damage from BC. Extreme ITCZ equatorward shift ( $\Delta\text{ITCZ} < -2.1^\circ$ ) had higher impacts on either mitigation or aggravation of BC-associated premature mortalities (i.e., reduced 14 percent of premature mortalities in the maritime area and increased 7 percent in the continental area). Supplementary Table 2 shows comparable results based on the population and mortality rate in 2015 from GBD dataset.

It suggests that ITCZ shift under climate change can threaten the continental countries by worsening the local dispersion condition, even though boreal summertime is typically not the main biomass burning season in this area. Under climate change, not only people living in regions with pronounced biomass burning (i.e., in the maritime area) will be threatened, but also people living in higher-latitude regions where emissions are relatively lower. It is noted that this study just focused on one kind of toxic air pollutant, and other species (e.g.,  $\text{PM}_{2.5}$ , organic carbon, and sulfate, etc.) in biomass burning events may make the risks even higher. Nevertheless, it should be noted that BC is relatively toxic among PM species<sup>33</sup>.

## Discussion

Our results suggest that recent equatorial warming induced by anthropogenic activities contributed to the equatorward shift ( $\sim 2.1^\circ$ ) of seasonal-mean zonal-mean ITCZ location in Maritime Continent. The equatorward shift enhanced updrafts, extra rainfall, and wet deposition over the maritime area, hence decreasing surface BC concentration. However, the equatorward shift increased BC concentration in the continental area by weakening updrafts. Meanwhile, anomalous low-level northeast wind induced by the equatorward shift weakened summer circulation and suppresses transboundary air pollution, leading to a decrease of BC concentration in the Philippines. Considering the adverse impact of BC on public health, the ITCZ shift also brought about different health impacts on each area in Maritime Continent by altering the distribution of BC under climate change.

We highlight the spatial heterogeneity of the impacts on BC and public health induced by equatorward ITCZ shift. In the Philippines, biomass burning emissions from the upwind region (i.e., Borneo) were another contributor to the surface BC concentration in the southern part of the Philippines under East Asia summer monsoon. We found that the equatorward shift of ITCZ weakened the circulation, suppressing the transport of pollutants to southern part of the Philippines. Advection changes in maritime and continental areas were not significant, but the vertical regulation of air pollution between ground and upper level was more remarkable. In the maritime area, the equatorward shift of ITCZ mitigated the severe BC pollution and the corresponding health risk, while people living in the continental area may hence suffer from additional health risk, especially when this shift may continue in the future along with the population growth in this area.

Even though we found the equatorward shift of ITCZ location in Maritime Continent, our analysis did not show any width changes of ITCZ belt, which is sometimes regarded as the extent of tropics. The width of ITCZ in Maritime Continent is not as easily defined as other regions over the oceans. Different definitions may result in the uncertainty of the trend. Also, ITCZ location shift cannot represent tropical expansion. The direction of Hadley cell, which is different from the concept of tropical expansion<sup>19,40</sup> that has been investigated comprehensively during the past decades. Typically, tropical expansion refers to the poleward extent of the descending branches of Hadley Cell in both hemispheres. The location of ITCZ does not necessarily determine the magnitude of Hadley cell and the position of descending area (i.e., often defined as the edge of the tropics), although the intensified ITCZ found

in this study might indicate a strengthened Hadley circulation that can extend further to the high-latitude areas. The shifts of ITCZ locations in the oceanic regions show a poleward shift due to the positive-to-negative PDO phase change but veer to the equator when positive PDO dominates in the future climate<sup>12</sup>, indicating that in Maritime Continent anthropogenic activities-induced equatorial warming may overwhelm the impacts of positive-to-negative PDO phase change, leading to an equatorward shift ITCZ and will continue in the future.

Despite the fact that our study demonstrates a clear equatorward shift of ITCZ location in Maritime Continent during the past 35 years, this trend requires further investigation using other datasets such as precipitation. Current long-term observational precipitation datasets generally have a coarse spatial resolution (e.g., GPCP data), which may not be able to fully detect the shift close to the model resolution. Also, the model bias in long-term precipitation simulations (i.e., double-ITCZ bias in CMIP5 and CMIP6)<sup>41–43</sup> also needs to be further corrected to provide trustworthy data for future analysis. Although our statistical study did not include the impact of daily scale BC perturbations such as aging or local wet deposition, the uncertainties from these processes may still exist and need to be evaluated in future research. In terms of the association between ITCZ and BC anomalies, even though we have applied monthly scale correlation analysis and composite analysis to avoid other long-term impacts such as interannual or decadal climate variabilities on BC concentration, quantitatively assessments based on numerical simulations are still required in the future research to further explain the mechanism.

In summary, we used multiple reanalysis datasets to explore the variation of seasonal-mean zonal-mean ITCZ location in Maritime Continent from 1980 to 2014. We found an equatorward shift of boreal summer ITCZ by  $\sim 2.1^\circ$  in recent ten years (2005–2014) compared with that in the historical period (1980–1989). Meanwhile, ITCZ intensity also increased. Recent equatorial warming, which was attributed to anthropogenic activities using multiple CMIP6 simulations, played a vital role in this shift. We further investigated the impact of ITCZ equatorward shift on surface BC concentration in three sub-areas in Maritime Continent using composite analysis. It reveals that enhanced updrafts, extra rainfall and wet deposition over maritime area resulted in the decrease in surface BC concentration, while the weakened updrafts elevated BC concentration in continental area when ITCZ shifted equatorward. Different from the mechanism of vertical atmospheric movement, anomalous low-level northeasterly wind weakened summer circulation, leading to a decrease in BC concentration in the Philippines. Overall, in boreal summer, the equatorward ITCZ shift decreased  $\sim 13\%$  of BC-associated monthly premature mortalities in maritime countries, but increased  $\sim 6\%$  of that in continental countries (2010 baseline). The impacts were magnified ( $-14\%$  in the maritime area and  $+7\%$  in the continental area) in an extreme ITCZ shift situation (i.e.,  $\Delta\text{ITCZ} < -2.1^\circ$ ).

## Methods

### ITCZ metrics

Three metrics (i.e., location, intensity and width) for the ITCZ were computed in ERA5, MERRA-2, NCEP-DOE and ERA-interim datasets according to the methods used in Zhou et al.<sup>1,12</sup>. The location of ITCZ was defined as the latitude of the peak ascent ( $\omega_{500}$ ) averaged over the corresponding longitude range, and the intensity was defined as the peak value of the ITCZ ascent ( $\omega_{500}$ ). The width of ITCZ was traditionally defined as the cartesian distance between the latitudes of zonal-mean seasonal-mean  $\omega_{500}$  lower than  $-15$  hPa per day. However, as the northern ITCZ boundary in Maritime Continent in boreal summer is not as clear as the southern one (See Supplementary Fig. 10, defined by traditional method), we obtained the width of ITCZ in Maritime Continent from:

$$\text{Width} = \frac{\text{Area}}{\text{Length}} \quad (1)$$

where *Area* is the area of grids with  $\omega_{500} < -15$  hPa per day, and *Length* is the longitude length of Maritime Continent (i.e., 70° in this study), referring to the definition applied to South Pacific ITCZ in ref. 12.

### Attribution of equatorial warming to anthropogenic activities

Attribution of equatorial warming to anthropogenic activities was performed based on CMIP6 models. The key process of the attribution was to use simulations of climate models to compare the differences in extreme weather or climate events under climate conditions that were affected and not affected by human activities<sup>44</sup>. To allow for the different model representations of the climate system, we used monthly surface air temperature generated by the 10 CMIP6 models (Supplementary Table 3) but based on two scenarios: All-Hist and Nat-Hist. The selection of models was dependent on the availability of both scenarios and the consistency of runs (r1i1p1f1). In the All-Hist scenario, simulations of surface air temperature were forced by historical anthropogenic and natural external forcing agents with observational data of SST and sea ice in CMIP6 models, whereas models forced by historical natural forcing only (e.g., solar and volcanic forcings) were selected as the Nat-Hist scenario<sup>45</sup>. The probability density function (PDF) of temperature anomalies derived from SST observation, All-Hist simulations and Nat-Hist simulations were calculated respectively. Comparison between PDF derived from simulations and from observation were conducted via the Kolmogorov–Smirnov (KS) test. Anthropogenic contributions can be detected if the p-value between All-Hist and observation was less than 0.05 while the p-value between Nat-Hist and observation was larger than 0.05.

### Composite analysis

To analyze the impacts of equatorward shift of ITCZ on BC and public health, we calculated the anomalies (i.e., the difference between the exact monthly record and the long-term mean of the record from 1980 to 2014) of BC, circulation, and premature mortalities in the corresponding months, and then averaged the anomalies. The significance of the changes was diagnosed by student's t-test.

### BC-associated health impact

In this study, the concentration-response function (CRF) derived from epidemiological research was utilized to estimate the number of all-age all-cause premature mortalities associated with BC exposure. In the detailed calculation, all-age all-cause premature mortalities under the exposure of ambient BC concentration were estimated by the function below that describes the log-linear relationship between population, baseline incident rate, and the health risk factor in each country with an unit increase of BC concentration<sup>34</sup>:

$$RR_k = e^{\gamma \cdot X_k} \quad (2)$$

$$E = \sum_k (RR_k - 1) / RR_k \cdot P_k \cdot f \quad (3)$$

where  $RR_k$  refers to the relative health risk of BC exposure, and  $k$  stands for each grid in the datasets.  $X_k$  is the monthly surface BC concentration in each grid from MERRA-2 dataset. Data validation can be found in Supplementary Method in SI.  $E$  is the final all-age all-cause premature mortalities.  $P$  is the population in each grid. The dataset of population from WorldPop has a spatial resolution of 100 m. The population was firstly aggregated to a resolution near BC dataset (0.5° × 0.5°), and then interpolated to match the exact resolution of BC (0.5° × 0.625°).  $f$  refers to the yearly all-age all-cause premature mortality rate derived from GBD in each country. To derive monthly mortality rate,  $f$  was divided by 12, inspired by the method for daily mortality rate in a previous study<sup>46</sup>.

In this study, the values of coefficient  $\gamma$  were retrieved from a meta-regression that pooled all-cause mortalities to BC concentration from

multiple cohorts and previous studies<sup>34,47</sup>. Uncertainties mainly came from the estimation of  $\gamma$  in the CRF. We used Monte-Carlo approach to investigate the uncertainty of human health results<sup>48</sup>. Based on the low (0.0023), median (0.0060) and upper values (0.0098) of  $\gamma$  derived from Gu et al. (2020), we assumed a triangular probability distribution and obtained 10,000  $\gamma$  estimations. Each estimated parameter was then regarded as an input into the estimation of premature mortalities. The ultimate range of uncertainty was expressed by the median value and 95% confidence interval (CI) of these 10,000 health impact results<sup>34</sup>.

### Data availability

$\omega_{500}$  product was derived from ERA5 (<https://cds.climate.copernicus.eu/cdsapp#!/dataset/reanalysis-era5-pressure-levels-monthly-means?tab=form>), MERRA-2 (<https://disc.gsfc.nasa.gov/datasets?project=MERRA-2>), NCEP-DOE (<https://psl.noaa.gov/data/gridded/data.ncep.reanalysis2.html>) and ERA-interim (<https://www.ecmwf.int/en/forecasts/dataset/ecmwf-reanalysis-interim>). Low-level circulation products were derived from ERA5 in this study. Surface BC concentration was obtained from MERRA-2. Nat-hist and All-hist simulations were obtained from 10 CMIP6 models (ACCESS-CM2, BCC-CSM2-MR, CanESM5, CESM2, E3SM-2-0, GFDL-ESM4, IPSL-CM6A-LR, MIROC6, MRI-ESM2-0 and NorESM2-LM, <https://esgf-node.llnl.gov/search/cmip6/>). Monthly precipitation record was obtained from Global Precipitation Climatology Project (GPCP, <https://climatedataguide.ucar.edu/climate-data/gpcp-monthly-global-precipitation-climatology-project>). Monthly SST dataset was from COBE Sea Surface Temperature data provided by the NOAA PSL, Boulder, Colorado, USA, from their website at <https://psl.noaa.gov>. Annual all-age all-cause premature mortality rate and population data were derived from Global Burden of Disease (<https://www.healthdata.org/gbd>).

### Code availability

The source codes for analyzing the reanalysis and model datasets in this study are available from the corresponding author upon reasonable request.

Received: 6 November 2023; Accepted: 14 February 2024;

Published online: 29 February 2024

### References

- Zhou, W., Xie, S.-P. & Yang, D. Enhanced equatorial warming causes deep-tropical contraction and subtropical monsoon shift. *Nat. Clim. Chang.* **9**, 834–839 (2019).
- Adam, O., Bischoff, T. & Schneider, T. Seasonal and Interannual Variations of the Energy Flux Equator and ITCZ. Part I: Zonally Averaged ITCZ Position. *J. Clim.* **29**, 3219–3230 (2016).
- Adam, O., Bischoff, T. & Schneider, T. Seasonal and Interannual Variations of the Energy Flux Equator and ITCZ. Part II: Zonally Varying Shifts of the ITCZ. *J. Clim.* **29**, 7281–7293 (2016).
- Wodzicki, K. R. & Rapp, A. D. Long-term characterization of the Pacific ITCZ using TRMM, GPCP, and ERA-Interim. *J. Geophys. Res. -Atmos.* **121**, 3153–3170 (2016).
- Pausata, F. S. R. & Camargo, S. J. Tropical cyclone activity affected by volcanically induced ITCZ shifts. *Proc. Natl Acad. Sci. U.S.A.* **116**, 7732–7737 (2019).
- Biasutti, M. & Voigt, A. Seasonal and CO2-Induced Shifts of the ITCZ: Testing Energetic Controls in Idealized Simulations with Comprehensive Models. *J. Clim.* **33**, 2853–2870 (2020).
- Donohoe, A., Marshall, J., Ferreira, D. & Mcgee, D. The Relationship between ITCZ Location and Cross-Equatorial Atmospheric Heat Transport: From the Seasonal Cycle to the Last Glacial Maximum. *J. Clim.* **26**, 3597–3618 (2013).
- Wang, F. et al. Controls on the Northward Movement of the ITCZ over the South China Sea in Autumn: A Heavy Rain Case Study. *Adv. Atmos. Sci.* **38**, 1651–1664 (2021).
- Mamalakis, A. et al. Zonally contrasting shifts of the tropical rain belt in response to climate change. *Nat. Clim. Chang.* **11**, 143–151 (2021).

10. Byrne, M. P. & Schneider, T. Narrowing of the ITCZ in a warming climate: Physical mechanisms. *Geophys. Res. Lett.* **43**, 11,350–11,357 (2016).
11. Watt-Meyer, O. & Frierson, D. M. W. ITCZ Width Controls on Hadley Cell Extent and Eddy-Driven Jet Position and Their Response to Warming. *J. Clim.* **32**, 1151–1166 (2019).
12. Zhou, W., Leung, L. R., Lu, J., Yang, D. & Song, F. Contrasting Recent and Future ITCZ Changes From Distinct Tropical Warming Patterns. *Geophys. Res. Lett.* **47**, e2020GL089846 (2020).
13. Lau, W. K. M. & Tao, W. Precipitation–Radiation–Circulation Feedback Processes Associated with Structural Changes of the ITCZ in a Warming Climate during 1980–2014: An Observational Portrayal. *J. Clim.* **33**, 8737–8749 (2020).
14. Donohoe, A., Atwood, A. R. & Byrne, M. P. Controls on the Width of Tropical Precipitation and Its Contraction Under Global Warming. *Geophys. Res. Lett.* **46**, 9958–9967 (2019).
15. Kushner, P. J., Held, I. M. & Delworth, T. L. Southern Hemisphere Atmospheric Circulation Response to Global Warming. *J. Clim.* **14**, 2238–2249 (2001).
16. Fu, Q., Johanson, C. M., Wallace, J. M. & Reichler, T. Enhanced Mid-Latitude Tropospheric Warming in Satellite Measurements. *Science* **312**, 1179–1179 (2006).
17. Hu, Y. & Fu, Q. Observed poleward expansion of the Hadley circulation since 1979. *Atmos. Chem. Phys.* **7**, 5229–5236 (2007).
18. Lu, J., Vecchi, G. A. & Reichler, T. Expansion of the Hadley cell under global warming. *Geophys. Res. Lett.* **34**, L06805 (2007).
19. Seidel, D. J., Fu, Q., Randel, W. J. & Reichler, T. J. Widening of the tropical belt in a changing climate. *Nat. Geosci.* **1**, 21–24 (2008).
20. Allen, R. J. A 21st century northward tropical precipitation shift caused by future anthropogenic aerosol reductions. *J. Geophys. Res. -Atmos.* **120**, 9087–9102 (2015).
21. Freitas, A. C. V., Aímola, L., Ambrizzi, T. & de Oliveira, C. P. Extreme Intertropical Convergence Zone shifts over Southern Maritime Continent. *Atmos. Sci. Lett.* **18**, 2–10 (2017).
22. Cox, P. M. et al. Increasing risk of Amazonian drought due to decreasing aerosol pollution. *Nature* **453**, 212–215 (2008).
23. Labe, Z., Magnusdottir, G. & Stern, H. Variability of Arctic Sea Ice Thickness Using PIOMAS and the CESM Large Ensemble. *J. Clim.* **31**, 3233–3247 (2018).
24. Balting, D. F., AghaKouchak, A., Lohmann, G. & Ionita, M. Northern Hemisphere drought risk in a warming climate. *npj Clim. Atmos. Sci.* **4**, 1–13 (2021).
25. Xian, P. et al. Smoke aerosol transport patterns over the Maritime Continent. *Atmos. Res.* **122**, 469–485 (2013).
26. Yamanaka, M. D. Physical climatology of Indonesian maritime continent: An outline to comprehend observational studies. *Atmos. Res.* **178–179**, 231–259 (2016).
27. Field, R. D., van der Werf, G. R. & Shen, S. S. P. Human amplification of drought-induced biomass burning in Indonesia since 1960. *Nat. Geosci.* **2**, 185–188 (2009).
28. Field, R. D. et al. Indonesian fire activity and smoke pollution in 2015 show persistent nonlinear sensitivity to El Niño-induced drought. *Proc. Natl Acad. Sci. U.S.A.* **113**, 9204–9209 (2016).
29. Koplitz, S. N. et al. Role of the Madden-Julian Oscillation in the Transport of Smoke From Sumatra to the Malay Peninsula During Severe Non-El Niño Haze Events. *J. Geophys. Res. -Atmos.* **123**, 6282–6294 (2018).
30. Kuwata, M., Miyakawa, T., Yokoi, S., Khan, M. F. & Latif, M. T. The Madden-Julian Oscillation Modulates the Air Quality in the Maritime Continent. *Earth Space Sci.* **8**, e2021EA001708 (2021).
31. Page, S. E. et al. The amount of carbon released from peat and forest fires in Indonesia during 1997. *Nature* **420**, 61–65 (2002).
32. Anderson, J. O., Thundiyil, J. G. & Stolbach, A. Clearing the Air: A Review of the Effects of Particulate Matter Air Pollution on Human Health. *J. Med. Toxicol.* **8**, 166–175 (2012).
33. Janssen, N. A. et al. *Health effects of black carbon*. (World Health Organization. Regional Office for Europe, 2012).
34. Gu, Y. et al. Assessing outdoor air quality and public health impact attributable to residential black carbon emissions in rural China. *Resour. Conserv. Recycle.* **159**, 104812 (2020).
35. Zelinsky, R. C., Zhang, C. & Liu, C. The Relationship between the ITCZ and MJO Initiation over the Indian Ocean. *J. Atmos. Sci.* **76**, 2275–2294 (2019).
36. Zhao, S. & Suzuki, K. Differing Impacts of Black Carbon and Sulfate Aerosols on Global Precipitation and the ITCZ Location via Atmosphere and Ocean Energy Perturbations. *J. Clim.* **32**, 5567–5582 (2019).
37. He, C. & Zhou, W. Different Enhancement of the East Asian Summer Monsoon under Global Warming and Interglacial Epochs Simulated by CMIP6 Models: Role of the Subtropical High. *J. Clim.* **33**, 9721–9733 (2020).
38. Liu, J., Xu, H. & Deng, J. Projections of East Asian summer monsoon change at global warming of 1.5 and 2 °C. *Earth Syst. Dynam.* **9**, 427–439 (2018).
39. Li, Z., Sun, Y., Li, T., Ding, Y. & Hu, T. Future Changes in East Asian Summer Monsoon Circulation and Precipitation Under 1.5 to 5 °C of Warming. *Earth Future* **7**, 1391–1406 (2019).
40. Grise, K. M. et al. Recent Tropical Expansion: Natural Variability or Forced Response? *J. Clim.* **32**, 1551–1571 (2019).
41. Adam, O., Schneider, T. & Brient, F. Regional and seasonal variations of the double-ITCZ bias in CMIP5 models. *Clim. Dyn.* **51**, 101–117 (2018).
42. Ahn, M.-S. et al. MJO Propagation Across the Maritime Continent: Are CMIP6 Models Better Than CMIP5 Models? *Geophys. Res. Lett.* **47**, e2020GL087250 (2020).
43. Ge, F., Zhu, S., Luo, H., Zhi, X. & Wang, H. Future changes in precipitation extremes over Southeast Asia: insights from CMIP6 multi-model ensemble. *Environ. Res. Lett.* **16**, 024013 (2021).
44. National Academies of Sciences, Engineering, and Medicine. *Attribution of Extreme Weather Events in the Context of Climate Change*. (National Academies Press). <https://doi.org/10.17226/21852>. (2016).
45. Gillett, N. P. et al. The Detection and Attribution Model Intercomparison Project (DAMIP v1.0) contribution to CMIP6. *Geosci. Model Dev.* **9**, 3685–3697 (2016).
46. Xiao, Q. et al. Tracking PM2.5 and O3 Pollution and the Related Health Burden in China 2013–2020. *Environ. Sci. Technol.* **56**, 6922–6932 (2022).
47. Achilleos, S. et al. Acute effects of fine particulate matter constituents on mortality: A systematic review and meta-regression analysis. *Environ. Int.* **109**, 89–100 (2017).
48. Yim, S. H. L. et al. Effect of Urbanization on Ozone and Resultant Health Effects in the Pearl River Delta Region of China. *J. Geophys. Res. -Atmos.* **124**, 11568–11579 (2019).

## Acknowledgements

This research is jointly supported by the Ministry of Education, Singapore, under its MOE AcRF Tier 3 Award MOET32022-0006, the Start-up Grant (021452-00001) (LKC) and Start-up Grant (021384-00001) for Assoc. Prof. Yim (ASE), the MOE Academic Research Fund (AcRF) Tier 1 Project (022713-00001) and EOS FY2022 funding (award no: EOS MOE RCE FY 2022). This work comprises EOS contribution number 576.

## Author contributions

Tao Huang: Investigation, Visualization, Analysis, Writing–Original draft, Reviewing, Editing. Yefu Gu: Methodology, Reviewing, Editing. David Lallemant: Methodology, Reviewing. Gabriel N.C. Lau: Writing, Reviewing, Editing. Joseph J.Y. Sung: Writing, Reviewing, Editing. Steve H.L. Yim: Investigation, Conceptualization, Analysis, Methodology, Writing, Reviewing, Editing, Supervision.

### Competing interests

The authors declare no competing interests.

### Additional information

**Supplementary information** The online version contains supplementary material available at

<https://doi.org/10.1038/s41612-024-00593-6>.

**Correspondence** and requests for materials should be addressed to Steve H. L. Yim.

**Reprints and permissions information** is available at <http://www.nature.com/reprints>

**Publisher's note** Springer Nature remains neutral with regard to jurisdictional claims in published maps and institutional affiliations.

**Open Access** This article is licensed under a Creative Commons Attribution 4.0 International License, which permits use, sharing, adaptation, distribution and reproduction in any medium or format, as long as you give appropriate credit to the original author(s) and the source, provide a link to the Creative Commons licence, and indicate if changes were made. The images or other third party material in this article are included in the article's Creative Commons licence, unless indicated otherwise in a credit line to the material. If material is not included in the article's Creative Commons licence and your intended use is not permitted by statutory regulation or exceeds the permitted use, you will need to obtain permission directly from the copyright holder. To view a copy of this licence, visit <http://creativecommons.org/licenses/by/4.0/>.

© The Author(s) 2024